

The impact of reflectance variation in silicon heterojunction solar cells and modules on the perception of color-differences

Kaifu Qiu, Karsten Bittkau, Andreas Lambertz, Weiyuan Duan, Zongcun Liang, Hui Shen, Uwe Rau, Kaining Ding

Abstract—The Color produced by visible light that reflects from the photovoltaic modules can influence visual aesthetics for colored photovoltaic applications, such as the building integrated photovoltaic and the vehicles integrated photovoltaic. How two colors lying close together can be perceived by the human eye is important for aesthetic design. In this work, we investigated the reflectance spectra variation caused by the variation of indium tin oxide thickness and incidence angle of sunlight based on the well-known silicon heterojunction solar cells and modules. By converting the reflectance spectra into the Delta E 2000 value, we quantify whether differences in color can be perceived. The colors were also predicted based on the standard Red, Green, and Blue color space. The results show that the reflectance variation due to an ITO thickness deviation of 5 nm in SHJ solar cells leads to a perceptible color difference, which can be suppressed after encapsulation but is still perceptible on close observation. ITO thickness deviation should be controlled within 3 nm to produce the nearly imperceptible visual appearance. The color difference of SHJ modules with an ITO thickness of 70 nm is nearly imperceptible if the incidence angle is below 70°. For comparison, the color differences of the passivated emitter and rear contact solar cells using SiN_x as an anti-reflection layer was also investigated.

Index Terms—silicon heterojunction solar cells, passivated emitter and rear contact solar cells, reflectance spectra, Delta E 2000, color difference perception

I. INTRODUCTION

PHOTOVOLTAIC (PV) becomes even more prominent under the background of climate changing. PV modules are usually used in ground-mounted solar power plants or rooftop PV installations to utilize the available area as much as possible. As another application of the PV technology, building integrated PV (BIPV) systems have attracted increasing interest in the past decade. In addition to BIPV, vehicles integrated PV (VIPV) emerges in recent years [1, 2]. Rooftop PV modules are generally not visible, but BIPV and

VIPV bring them on an equal footing, increasing interests in the visual aesthetics of PV modules. The color of an opaque solar cell, such as crystalline silicon solar cell [3], CIGS solar cell [4], or CdTe solar cell [5], is produced by visible (VIS) sunlight that reflects from the cell and can be partially controlled by modifying the thickness of the anti-reflection coating (ARC) [6]. In addition, the optical appearance of opaque solar cells can be further modified by applying colored optical coatings to the front glass [7] or the encapsulation polymer layer [5]. Spatial variation in the ARC thickness might lead to undesired inhomogeneity in optical appearance, besides optical losses in solar cell efficiency. Thus, it is important for the PV manufacturers to predict the color of a cell and a module, and to determine whether to set tolerances to the acceptable color variation or to optimize the process condition to obtain a particular color.

An initial investigation of the colors and efficiency of solar cells as a function of the thickness of the silicon nitride (SiN_x) ARC was reported by Mason et al. [8] in 1995. T. M. Bruton et al. [9] reported a work to understand and control the process that affects the thickness and hence color of the SiN_x ARC in 2007. From 2011 to 2018, several studies predicted the color from the respective of the surface structure, illumination spectrum, scattering, observer angle of solar cells before and after encapsulation based on single SiN_x ARC or SiO₂/SiN_x double ARC [3, 10, 11]. Silicon heterojunction (SHJ) solar cells with indium tin oxide (ITO) as ARC become more and more popular among the PV industry due to the high efficiency, lean process, low-temperature coefficient and low degradation, which leads to increasing applications of the SHJ PV module. However, to the authors' knowledge, the investigations of color variation in the SHJ solar cells and modules, and the perception of the color differences have been missing.

In this paper, we investigated the variation of reflectance spectra caused by different ARC thicknesses and angles of

The work is supported with the HEMF (Helmholtz Energy Materials Foundry) infrastructure funded by the (HGF) Helmholtz association, the National Natural Science Foundation of China (Grant No.61774173), the Guangzhou collaborative innovation Major Project for producing, teaching and researching (Grant No. 201508010011) and the Jiangsu Collaborative Innovation Center of Photovoltaic Science and Engineering (Grant No. SCZ1405500002).

K. Qiu is with School of Physics, Sun Yat-Sen University, Guangzhou, 510275, PR China and also with IEK-5 Photovoltaik, Forschungszentrum Jülich, 52428 Jülich, Germany (e-mail: qiukaifu@outlook.com).

K. Bittkau, A. Lambertz, W. Duan, Uwe. Rau and K. Ding are with IEK-5 Photovoltaik, Forschungszentrum Jülich, 52428, Germany (e-mail: k.bittkau@fz-juelich.de, a.lambertz@fz-juelich.de, w.duan@fz-juelich.de, uwe.rau@fz-juelich.de, k.ding@fz-juelich.de).

Z. Liang and H. Shen are with School of Physics, Sun Yat-Sen University, Guangzhou, 510275, PR China and with Institute for Solar Energy Systems, Guangdong Provincial Key Laboratory of Photovoltaic Technology, Sun Yat-Sen University, Guangzhou, 510004, PR China, and also with State Key Laboratory of Optoelectronic Materials and Technologies, Sun Yat-Sen University, Guangzhou, PR China (e-mail: liangzc@mail.sysu.edu.cn, shenhui1956@163.com).

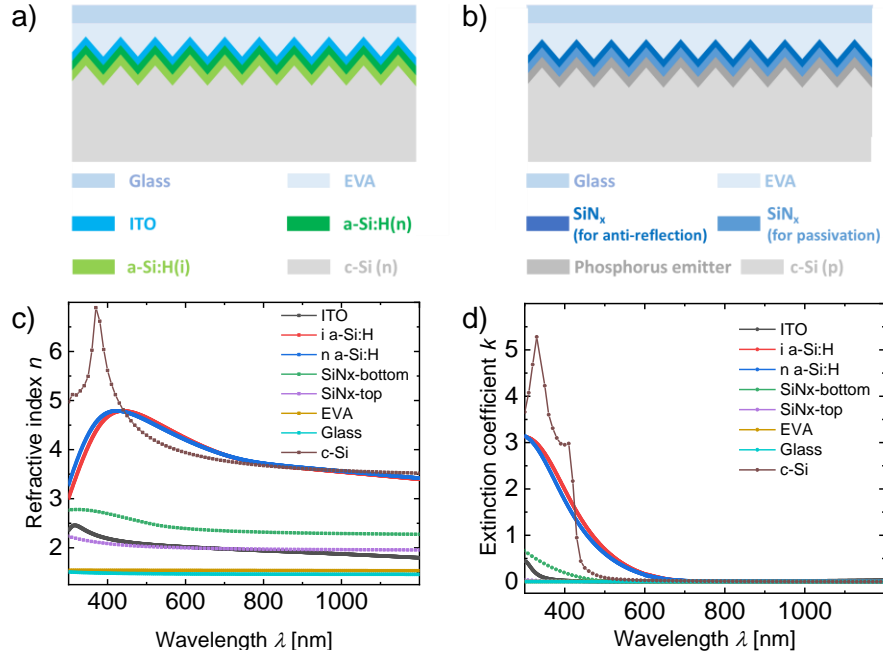


Fig. 1. The front side schematic diagram of the module based on (a) SHJ solar cells and (b) PERC solar cells. The thickness of EVA and glass used in both cases are 100 μm and 700 μm , respectively. There is no air gap assumed. The reflectivity at the air/glass interface has been subtracted from the simulations to get just the light that is reflected by the solar cell. The layer optical properties of (c) refractive index and (d) extinction coefficient used in the simulations.

incidence of sunlight for SHJ solar cells by optical simulations. The thickness variation is relevant for all colored PV applications, to avoid a spotty facade on vehicle or building surface. Angle dependence is especially important for vehicles where the surfaces are curved and is also relevant for BIPV where building facade elements can have different orientations, depending on the building's architectural design. The perception of the color difference induced by reflectance variation was also discussed.

Furthermore, solar cells after encapsulation with an Ethylene-vinyl Acetate (EVA) layer and glass were investigated. The color of the solar cells and modules were also predicted based on the standard Red, Green, and Blue (sRGB) color space. As a comparison, the same methodology was applied to determine whether the color differences of the passivated emitter and rear contact (PERC) solar cells using SiN_x as an anti-reflection layer can be perceived.

Previous works reported colored modules by using the Morpho butterfly effect, a bionic concept based on 3D photonic structures [12] or using integrated resonant dielectric nanoscatterers [13]. In our work, no special structures were involved to achieve a much broader range of colors, since the focus of this work is to propose a method to investigate the color differences of solar cells and modules, that applies a lean process. With the color prediction, SHJ manufactures can avoid costly experiments when (i) forecasting the cell color change after encapsulation, (ii) optimizing for a particular color for VIPV or BIPV applications, and (iii) determining the production tolerances to limit color variability within a cell or module.

II. MODEL AND METHOD

A non-metallized front side structure of ITO/a-Si:H(n/i)/c-Si for the SHJ solar cells and SiN_x/c-Si for the PERC solar cells were used in the simulation, respectively. A 100 μm thick EVA and a 700 μm thick glass were used for encapsulation, as shown in Fig. 1(a) and Fig. 1(b). A double layer of SiN_x was applied for the sake of optimal combination of passivation and anti-reflection for PERC solar cells, of which the bottom SiN_x layer with refractive index (n) of 2.37 at 632 nm and constant thickness of 12 nm was used for passivation while the top SiN_x layer with n of 1.99 at 632 nm was used as the anti-reflection coating. To measure the n and extinction coefficient (k), intrinsic and phosphorus doped hydrogenated amorphous Si (a-Si:H) were deposited on the double-side polished (111) crystalline Si (c-Si) by plasma-enhanced chemical vapor deposition (PECVD), and ITO was deposited on glass by sputtering. Spectroscopic ellipsometry and Photothermal Deflection Spectroscopy (PDS) were used to measure the n & k value of a-Si:H and ITO. The n & k value of c-Si [14], top and bottom SiN_x [15], EVA [16] and glass [17] are taken from literatures. Figure 1(c) and Fig. 1(d) show the n & k values for these materials.

AM 1.5G spectrum was used for the simulation. This work does not consider the reflectance for specific observation and acceptance angles. The optical simulator called OPAL2 [18] was used to simulate the hemispherical reflectance from the front surface of the solar cells without encapsulation. Random upright pyramids with a facet angle of 54.74° were applied during the simulation. For modules encapsulated with EVA+glass, Sentaurus TCAD [19] using ray tracing method was employed, applying the transfer matrix method boundary

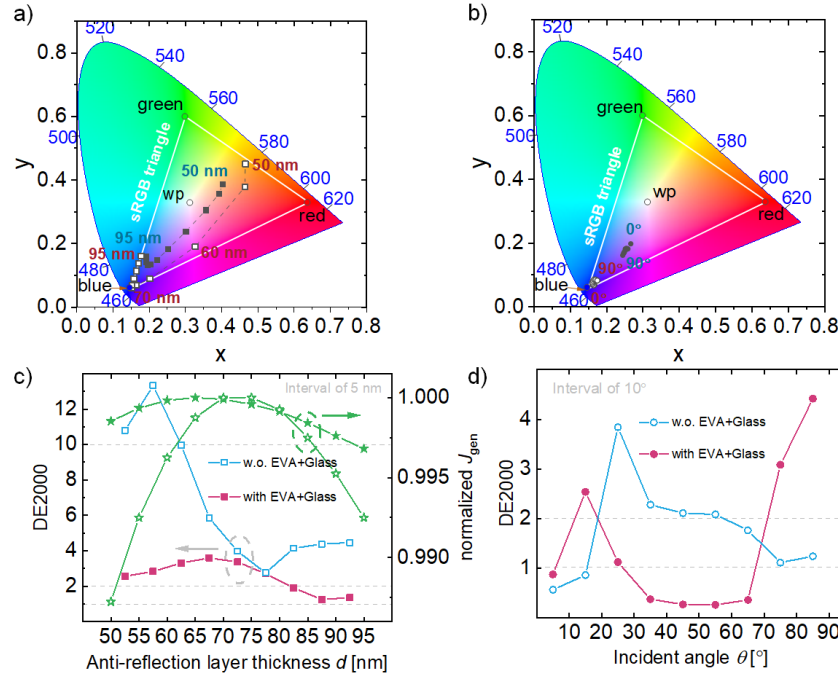


Fig. 2. Simulated xy points for the SHJ solar cells before (hollow) and after (solid) encapsulation with (a) ITO thickness of 50-95 nm and (b) angle of incidence of 0-90°, assuming a luminosity of $Y = 1$. The white point (wp) is that for the D65 6504 K spectrum and has xy coordinates of {0.31271, 0.32903}. The sRGB triangle covers the sRGB color space, each corner of the triangle is a primary: Red-{0.640, 0.330}, Green-{0.300, 0.600}, Blue-{0.150, 0.060}. Colors outside the triangle cannot be represented in RGB space by a standard computer monitor. The DE2000 values of two solar cells for comparison before (hollow) and after (solid) encapsulation with (c) ITO thickness with interval of 5 nm at normal incidence (the generated current density (J_{gen}) for the SHJ solar cells before (hollow) and after (solid) encapsulation as a function of ITO thickness is also shown. The J_{gen} is calculated over the whole wavelength ranging from 300 nm to 1200 nm and normalized to the maximum of the curve), and (d) angle of incidence with interval of 10° for an ITO thickness of 70 nm. For each DE2000 data point, the abscissa represents the mean value of the thickness or angle of incidence of two cells or modules used for comparison (The methodology is also adopted in the following graphs of DE2000).

condition between wafer and EVA to account for the thin layers. We calculated the hemispherical reflectance that excludes the direct reflectance at the air/glass interface [11], [18].

Sentaurus TCAD was used since a planar glass on a textured surface is not conformal and OPAL2 is not able to simulate an unconformable structure with multi-interfaces. Surface morphology determined from the confocal microscope based on the textured c-Si (100) was used as the input for TCAD simulation. The reflectance of the two types of solar cells was varied by varying the thickness of the ITO layer and the second SiN_x layer, respectively. For the sunlight incidence angle simulation, the azimuth angle was kept at 0° while varying the zenith angle to the normal of the plane of the cell from 0° to 90°.

The reflectance spectra were taken to multiply the spectrum by standard observer color matching functions to determine XYZ tri-stimulus values [20]. Only the light with wavelengths ranging from 360 nm to 830 nm has a contribution to color according to the color-matching functions of the CIE standard observer [21]. Although OPAL2 calculates the reflectance from a single interface, we can still use OPAL2 to determine the color of unencapsulated cells, as for the given wafer thickness, the reflectance of the entire solar cell is sufficiently described by the reflectance at the front interface in that wavelength range.

To facilitate the comparison of the different colors at equal

luminosity (Y-value), we presented the results on the CIExyY chromaticity chart by linear scaling XYZ to give a luminosity of $Y=1$, where the xy coordinates of the white point (WP) were {0.31271, 0.32903}. For better visualization, the XYZ coordinates were further transformed into the sRGB color

TABLE I
DELTA E VALUE AS A GENERAL GUIDE FOR VISUAL PERCEPTION

Delta E	PERCEPTION
≤ 1.0	Not perceptible by human eyes
1-2	Perceptible through close observation
2-10	Perceptible at a glance
11-49	Colors are more similar than opposite
100	Colors are exact opposite

space. Processing images in the sRGB color profile ensures accurate colors across multiple computer monitor. Finally, the sRGB values of two solar cells were used as inputs for an online Delta E 2000 (DE2000) calculator [22, 23] to calculate the DE2000 values [24], which is currently the most accurate CIE color difference algorithm available, and by far the most widely used formula [25], to understand how to perceive the color differences between two solar cells and modules with different reflectance. Table I shows the Delta E values as a general guide for visual perception [26].

III. RESULT AND DISCUSSION

A. The Impact of ITO Thickness and Angle of Incidence on The Color Difference

ITO thickness was varied from 50 nm to 95 nm with an interval of 5 nm while the thickness of intrinsic a-Si:H and n-type a-Si:H were both kept at 5 nm, as the reflectance spectra are most sensitive to ITO thickness variation rather than the a-Si:H layer thicknesses. The ITO thickness range specified here was intended to ensure the high performance of the solar cells. For the incidence angle series, we varied the zenith angle of the incident light from 0° to 90° with an interval of 10° while keeping the azimuth angle at 0°. The thicknesses of ITO, intrinsic a-Si:H and n-type a-Si:H were kept at 70 nm, 5 nm and 5 nm, respectively.

Figure 2(a) and Fig. 2(b) show the dependency of the colors of the solar cells and modules on the variation of the ITO thickness and the angle of incidence, respectively, by using the simulated xy points and assuming a luminosity of $Y = 1$.

Figure 2(a) shows that small changes in ITO thickness before encapsulation lead to significant color variation of the solar cell. The color gradually changes from brown to light purple, purple and dark blue to light blue as the ITO thickness increases from 50 nm to 95 nm. After encapsulation, however, these color differences are suppressed and the red contribution decreases with thinner ITO due to the lower reflectance at long wavelengths, while the blue contribution decreases with thicker ITO due to the lower reflectance at short wavelengths.

To determine the color difference for two solar cells or modules with an ITO thickness deviation of 5 nm, DE2000 values were calculated and plotted as a function of ITO thickness, as shown in Fig. 2(c). For each data point, the abscissa represents the mean value of the two cells used for comparison (for example, the abscissa of 52.5 nm means that the two compared samples have an ITO thickness of 50 nm and 55 nm). Regardless of whether the solar cells were encapsulated or not, all DE2000 values are greater than 1, which means that the color difference can be perceived. Especially for the DE2000 value above 2, human eye can see the color difference at a glance.

For the solar cells without encapsulation, the DE2000 value reaches the minimum value for solar cells with an ITO thickness of 75 nm and 80 nm, which allows the highest generated current density (J_{gen}), as shown by the J_{gen} curve in Fig. 2(c), which was normalized to the maximum. For ITO thicknesses below or above 75-80 nm, the higher DE2000 values indicate that the color differences are clearer. However, the DE2000 values show a stronger dependence on the ITO thickness below 75-80 nm than above, as the reflectivity changes significantly in this ITO thickness range.

Similar to the CIExyY chromaticity chart, the DE2000 values decreased after encapsulation, which is consistent with the suppression of color differences. Interestingly, the DE2000 value shows an opposite trend to that before encapsulation, which shows that the reflectance variation with thickness is different for solar cells and modules. However, only the modules with an ITO thickness larger than 80 nm and a thickness deviation within 5 nm showed a DE2000 value ranging from 1 to 2, which indicates the barely perceptible color difference, except by close observation. The modules with ITO thickness lower than 80 nm and thickness deviation over 5 nm lead to noticeable color differences at a glance.

The simulated, normalized J_{gen} of the modules is also shown in Fig. 2(c), which shows that an ITO thickness around 65 nm enables the best optical performance, but also leads to a relatively high DE2000 value. A shift of the optimal ITO thickness enabling the highest J_{gen} , from around 75 nm to 65 nm, was found after encapsulation, which indicates the different reflection mechanism behind. Besides, it was clearly shown that the dependence of J_{gen} on ITO thickness is greatly decreased after encapsulation.

Figure 2(b) shows that big changes in the angle of incidence don't lead to significant color variations for the solar cells. After encapsulation, however, the color differences are slightly enhanced.

Since direct reflection at the air/glass interface was excluded during the TCAD simulation, a simulated xy point closer to the white point is not found at large angles of incidence, which eliminates the so-called 'glare' effect, as shown in Reference [11], 'because the direct sunlight is reflected from the glass into the observer's eyes. Due to the





Thickness	50 nm	55 nm	60 nm	65 nm	70 nm	75 nm	80 nm	85 nm	90 nm	95 nm
Before encapsulation										
	(45,32,4)	(38,18,9)	(27,4,26)	(18,0,46)	(10,0,67)	(2,0,86)	(0,7,102)	(0,25,115)	(0,41,125)	(0,55,132)
After encapsulation										
	(24,18,13)	(20,13,13)	(16,9,15)	(12,7,20)	(10,5,26)	(8,5,33)	(7,6,40)	(7,8,46)	(6,13,51)	(4,18,56)
Incident angle	0°	10°	20°	30°	40°	50°	60°	70°	80°	90°
Before encapsulation										
	(10,0,67)	(12,0,69)	(14,0,72)	(18,0,92)	(17,5,106)	(16,14,118)	(20,21,129)	(27,26,139)	(35,24,144)	(43,18,144)
After encapsulation										
	(10,5,26)	(9,4,24)	(7,4,17)	(7,3,20)	(7,3,21)	(7,3,22)	(8,4,23)	(8,4,22)	(5,2,14)	(0,0,1)

Fig. 3. The predicted color for SHJ solar cells before and after encapsulation with different anti-reflection layer thickness at normal incidence and with different incidence angles for an ITO thickness of 70 nm. AM1.5g spectrum was used in the TCAD simulation. For solar cells after encapsulation, the reflectance at the air/glass interface is excluded. The provided numbers show the RGB values ranging from 0-255.

broadband nature of the glass reflectance, the observer is effectively seeing the sun's reflectance'.

DE2000 values of two solar cells and modules as a function of angle of incidence with an interval of 10° were calculated and shown in Fig. 2(d). For the solar cells without encapsulation, angles of incidence below 20° result in an imperceptible color difference, while angles of incidence from 20° to 40° show a perceptible color difference at a glance, and for the angles beyond 40° , the difference can be perceived by close observation.

The color difference for modules shows a different trend. The modules look similar if the angle of incidence remains below 70° , except for the angle of incidence changing from 10° to 20° . However, the DE2000 value increases significantly with increasing angle of incidence beyond 70° , indicating the more distinct color difference.

B. Predicted Color of SHJ Solar Cell and Module

As shown in Fig. 2(a) and Fig. 2(b), the simulated xy points, which assume a luminosity of $Y = 1$, are all located within the sRGB triangle, indicating that all these colors determined from the simulation can be displayed on a standard computer monitor. The CIExyY chromaticity chart shows how the color varies with changes in the anti-reflection layer thickness and angle of incidence. However, since a constant luminosity was assumed, not the 'actual color' is presented.

To this end, the color of the SHJ solar cells and modules were predicted by converting the reflectance spectra into sRGB value and demonstrated in the sRGB color space, as shown in Fig. 3. The corresponding (R, G, B) values for each predicted color are shown in brackets for better understanding.

From the predicted color, it can be clearly seen that the

modules, regardless of the ITO thickness series or angle of incidence series, become darker and thus show a less noticeable color difference. However, the color variation in the ITO thickness series still can be perceived. The solar cells with ITO thickness around 70-75 nm appear as dark blue solar cells after encapsulation, which agrees with reality. For the angle of incidence series, most of the color differences of the module cannot be perceived, except for angle of incidences larger than 70° . This behavior follows the results from the DE2000 calculations in Fig. 2.

For solar cells without encapsulation in the angle of incidence series, increasing the angle of incidence increases the red contribution and makes the color appear increasingly purple. For modules, however, the light intensity impinging the silicon surface is strongly decreased at large angles of incidence, since the light is reflected at the air/glass interface. As this directly reflected light is not considered as being detected by the observer's eye, the module appears darker at larger angles of incidence.

C. Comparison between SHJ and PERC module

Here, we included the currently common PERC modules and calculated the DE2000 values, and then compared these with those of SHJ modules. The reflectance spectra of different anti-reflection layer thicknesses can be found in Fig. 4(a). The reflectance in the range from 360 nm to 830 nm shows similar behavior for SHJ and PERC modules, but the PERC module shows a lower reflectance due to the superior property of SiN_x in terms of anti-reflection. As a result, the PERC module had a higher color difference tolerance for a thickness deviation of 5 nm, as shown in Fig. 4(b). In the PERC module, only the modules with a SiN_x thickness within 65-75 nm showed a perceptible color difference at a glance. For other thicknesses, the color differences were hardly

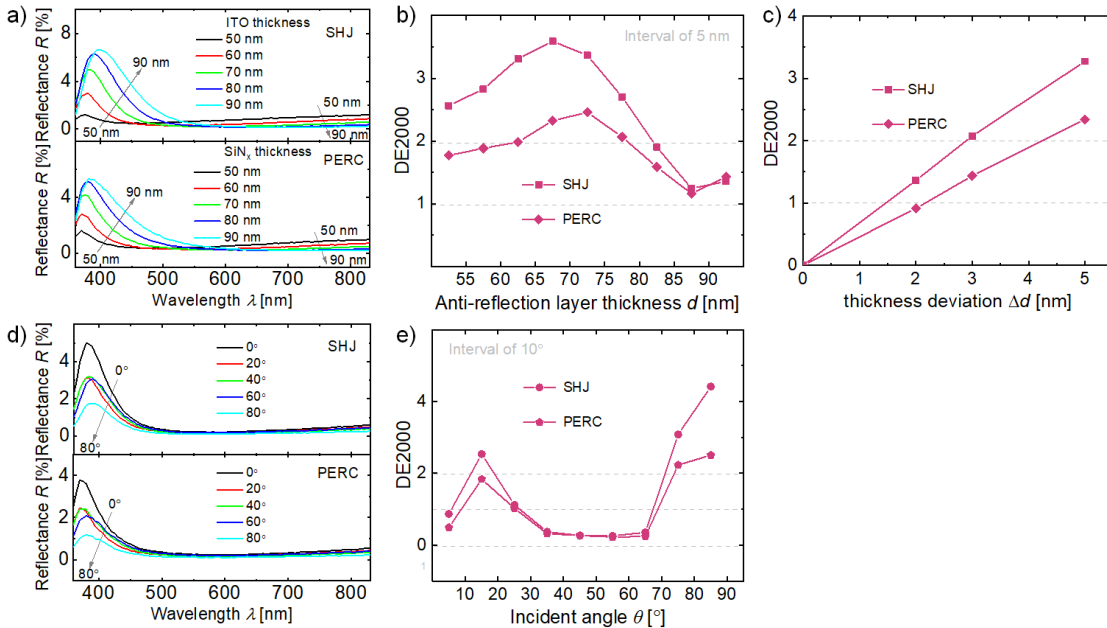


Fig. 4. The reflectance spectra as a function of (a) anti-reflection layer thickness at normal incidence and (d) incidence angles for SHJ and PERC module for anti-reflection layer thicknesses of 70 nm and 67 nm, respectively. The corresponding DE2000 value for pairs of modules with (b) different anti-reflection layer thickness and (e) different incidence angle for SHJ and PERC module. (c) DE2000 values as a function of thickness deviation for SHJ and PERC modules, with respect to the layer thickness (from 60 nm to 65 nm) around the highest J_{gen} .

noticeable without close observation. The sensitivity of the color difference on the layer thickness variation with respect to the layer thickness (from 60 nm to 65 nm) around the highest J_{gen} is shown in Fig. 4(c). In order to create a homogeneous visual appearance at a glance, the antireflection layer thickness should be controlled within 4 nm for PERC module and 3 nm for SHJ module, which is difficult for current ITO deposition systems for mass production, as the homogeneity within single wafer and single carrier are above $\pm 4\%$, i.e. thickness deviation of more than 5.2 nm for 65 nm ITO deposition.

Concerning the angle of incidence series, increasing the angle of incidence lead to lower reflectance. The reduction in reflectance was stronger at angles of incidence from 0° to 20° and at angles greater than 60° , as visualized in Fig. 4(d), resulting in greater color variation, as shown by the DE2000 values in Fig. 4(e). The color difference as a function of the angle of incidence for SHJ modules and PERC modules is more similar compared to the anti-reflection thickness series, which shows that both technologies exhibit good visual appearance tolerance when the angle of incidence of sunlight is varied. But PERC module still shows slightly better performance, especially if the angle of incidence is larger than 70° .

IV. CONCLUSION

An investigation is presented on how to perceive reflectance variation-induced color difference, based on today's popular SHJ and PERC technologies. The variation of the reflectance spectra by changing the thickness of the anti-reflection layer and the angle of incidence were determined by optical simulations. The results show that the reflectance variation in SHJ solar cells caused by ITO thickness deviation of 5 nm leads to a wide color range that can be suppressed after encapsulation, but the color difference is still perceptible on close observation. The ITO thickness deviation should be controlled within 3 nm to achieve a homogeneous visual appearance for SHJ modules. The comparison between the PERC and SHJ modules shows that PERC modules show a higher visual appearance tolerance under the condition of varying the anti-reflection layer thickness. For the condition of incidence angle variation, however, they show similar behavior, where angles of incidence below 70° allow a hardly noticeable color difference. This work gives some guidance for the visual aesthetical design of the increasingly popular BIPV or VIPV.

REFERENCES

- [1] Y. Lethwala, "Development of Auxiliary Automobile Air Conditioning System by Solar Energy", *International Research Journal of Engineering and Technology*, vol. 04, no. 07, pp. 737-742, 2017.
- [2] M. G. "First Ride: Lightyear One solar car gets 450 miles on 60kWh, even when sun isn't shining." <https://electrek.co/2020/01/14/lightyear-one-first-look/>
- [3] J. H. Selj, T. T. Mongstad, R. Søndena, and E. S. Marstein, "Reduction of optical losses in colored solar cells with multilayer antireflection coatings," *Solar Energy Materials and Solar Cells*, vol. 95, no. 9, pp. 2576-2582, 2011.
- [4] G. Y. Yoo *et al.*, "Multiple-Color-Generating Cu(In,Ga)(S,Se)₂ Thin-Film Solar Cells via Dichroic Film Incorporation for Power-Generating Window Applications," *ACS Applied Materials & Interfaces*, vol. 9, no. 17, pp. 14817-14826, 2017.
- [5] E. Klampaftis, D. Ross, and B. S. Richards, "Color, graphic design and high efficiency for photovoltaic modules," in *2014 IEEE 40th Photovoltaic Specialist Conference (PVSC)*, 8-13, 2014, pp. 0025-0029, doi: 10.1109/PVSC.2014.6925025.
- [6] I. Tobias, A. E. Moussaoui, and A. Luque, "Colored solar cells with minimal current mismatch," *IEEE Transactions on Electron Devices*, vol. 46, no. 9, pp. 1858-1865, 1999.
- [7] S. Pélisset *et al.*, "Efficiency of silicon thin-film photovoltaic modules with a front coloured glass," 2011. [Online]. Available: http://infoscience.epfl.ch/record/170333/files/paper_617.pdf.
- [8] N. B. Mason, "High efficiency production silicon solar cells with screen printed contacts," in *13th European Photovoltaic Solar Energy Conference*, Nice, 1995, pp. 2218 - 2219.
- [9] S. Roberts, A. Cole, K. Heasman, S. Devenport, M. Brown, and T. Bruton, *PROCESS DEVELOPMENT OF COLOURED LGBC SOLAR CELLS FOR BIPV APPLICATIONS*. 2007.
- [10] Y. Chen, Y. Yang, Z. Feng, P. Altermatt, and H. Shen, *Color modulation of c-Si solar cells without significant current-loss by means of a double-layer anti-reflective coating*. 2012.
- [11] K. R. McIntosh, M. Amara, F. Mandorlo, M. D. Abbott, and B. A. Sudbury, "Advanced simulation of a PV module's color," *AIP Conference Proceedings*, vol. 1999, no. 1, p. 020017, 2018.
- [12] B. Bläsi *et al.*, *MORPHO BUTTERFLY INSPIRED COLOURED BIPV MODULES*. 2017.
- [13] V. Neder, S. L. Luxembourg, and A. Polman, "Efficient colored silicon solar modules using integrated resonant dielectric nanoscatterers," *Applied Physics Letters*, vol. 111, no. 7, p. 073902, 2017, doi: 10.1063/1.4986796.
- [14] M. A. Green, "Self-consistent optical parameters of intrinsic silicon at 300K including temperature coefficients," *Solar Energy Materials and Solar Cells*, vol. 92, no. 11, pp. 1305-1310, 2008.
- [15] S. Duttgupta, F. Ma, B. Hoex, T. Mueller, and A. G. Aberle, "Optimised Antireflection Coatings using Silicon Nitride on Textured Silicon Surfaces based on Measurements and Multidimensional Modelling," *Energy Procedia*, vol. 15, pp. 78-83, 2012.
- [16] K. R. McIntosh, J. N. Cotsell, J. S. Cumpston, A. W. Norris, N. E. Powell, and B. M. Ketola, "An optical comparison of silicone and EVA encapsulants for conventional silicon PV modules: A ray-tracing study," in *2009 34th IEEE Photovoltaic Specialists Conference (PVSC)*, 7-12 June 2009 2009, pp. 000544-000549.
- [17] E. Raoult *et al.*, *Optical Characterizations and Modelling of Semitransparent Perovskite Solar Cells for Tandem Applications*. 2019.
- [18] K. R. McIntosh and S. C. Baker-Finch, "OPAL 2: Rapid optical simulation of silicon solar cells," in *2012 38th IEEE Photovoltaic Specialists Conference*, 3-8 June 2012 2012, pp. 000265-000271, doi: 10.1109/PVSC.2012.6317616.
- [19] Y.C. Wu and Y.R. Jhan, "Introduction of Synopsys Sentaurus TCAD Simulation," in *3D TCAD Simulation for CMOS Nanoelectronic Devices*. Singapore: Springer Singapore, 2018, pp. 1-17.
- [20] D. Malacara, "Color Vision and Colorimetry: Theory and Applications, Second Edition," 2011.
- [21] "Colour Matching Functions." [Online]. Available: <http://cvrl.ioo.ucl.ac.uk/cmfs.htm>.
- [22] Colormine.org. "CIE2000 Calculator." [Online]. Available: <http://colormine.org/delta-e-calculator/cie2000>
- [23] ColorTell©2019. "Colortool." [Online]. Available: <https://www.colortell.com/colortool>
- [24] W. Mokrzycki and M. Tatol, "Color difference Delta E - A survey," *Machine Graphics and Vision*, vol. 20, pp. 383-411, 04/01 2011.
- [25] A. Lakacha. "A simple review of CIE ΔE^* (Color Difference) Equations." <https://www.techkonusa.com/a-simple-review-of-cie-delta-e-color-difference-equations/>
- [26] Z. Schuessler. "Defining Delta E." [Online]. Available: <http://zschuessler.github.io/DeltaE/learn/>